

AD-A169 473

MEDIUM- AND LONG-WAVELENGTH INFRARED EMISSION FROM A
LASER-PRODUCED OXYGEN PLASMA(U) AIR FORCE GEOPHYSICS

1/1

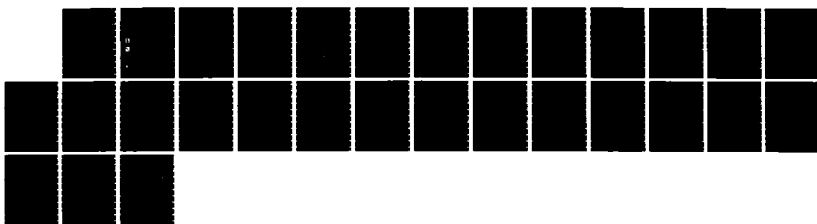
UNCLASSIFIED

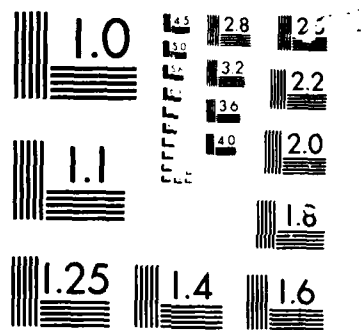
AFGL-TR-0341

LAB HANSCOM AFB MA J B LURIE ET AL. 31 DEC 85

F/G 20/9

NL





AFGL-TR-85-0341
ENVIRONMENTAL RESEARCH PAPERS, NO. 942

12

Medium- and Long-Wavelength Infrared Emission From a Laser-Produced Oxygen Plasma

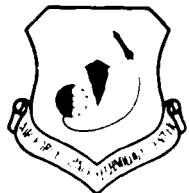
JONATHAN B. LURIE
JAMES C. BAIRD



31 December 1985



Approved for public release; distribution unlimited.



INFRARED TECHNOLOGY DIVISION
AIR FORCE GEOPHYSICS LABORATORY
PROJECT 2310
HANSCOM AFB, MA 01731

DTIC
SELECTED
JUL 1 1986
S B

86 7 1 066

This technical report has been reviewed and is approved for publication

Laila Dzelzkalns
LAILA DZELZKALNS
IHWI Scientist

W. Blumberg
W. BLUMBERG, Acting Chief
Infrared Dynamics Branch

FOR THE COMMANDER

Randall E. Murphy
RANDALL E. MURPHY, Director
Infrared Technology Division

This report has been reviewed by the ESD Public Affairs Office (PA) and is releasable to the National Technical Information Service (NTIS).

Qualified requestors may obtain additional copies from the Defense Technical Information Center. All others should apply to the National Technical Information Service.

If your address has changed, or if you wish to be removed from the mailing list, or if the addressee is no longer employed by your organization, please notify AFGL/DAA, Hanscom AFB, MA 01731. This will assist us in maintaining a current mailing list.

Do not return copies of this report unless contractual obligations or notices on a specific document requires that it be returned.

Unclassified

SECURITY CLASSIFICATION OF THIS PAGE

AD-5.69475

REPORT DOCUMENTATION PAGE

DD FORM 1473, 83 APR

EDUCATIONAL PLANNING FOR THE FUTURE

Non-classified

Acknowledgements

The authors gratefully acknowledge the support of the Air Force Office of Scientific Research and the Defense Nuclear Agency.

DTIC
ELECTE
S JUL 1 1986 D
B



Accepted

✓

DTIC

A-1

Contents

1. INTRODUCTION	1
2. EXPERIMENTAL	2
3. RESULTS	3
4. DISCUSSION	4
4.1 Linewidth	6
4.2 Stark Lineshape Theory	8
REFERENCES	23

Illustrations

1. Experimental Apparatus for Infrared Emission Studies	13
2. 5.5μ - 8μ Emission Spectrum of a 150 Torr Laser-Produced Oxygen Plasma With a $10\ \mu\text{s}$ Delay	14
3. 7.43μ Emission Linewidth vs Total Oxygen Pressure at $\tau_D = 6\mu\text{s}$	15
4. 7.43μ Emission Linewidth vs τ_D at 176 Torr Oxygen Pressure	16
5. 7.43μ Emission Line Area vs Total Oxygen Pressure at $\tau_D = 6\mu\text{s}$	17
6. 7.43μ Emission Line Area vs τ_D at Total Oxygen Pressure of 176 Torr	18

Illustrations

7. Simulated Emission Spectrum in the 5.5μ - 8.0μ Region Using Coulomb Approximation Intensities, 40 cm^{-1} Widths for the 6g and 6h States and 12 cm^{-1} Linewidths for the Rest of the Transitions	19
8. Synthetic Spectrum of 5.5μ - 8μ Emission Region for a Stark Field Corresponding to 10^{14} e's/cm ³ , a 6g - 5f, 6h - 6g Component Linewidth of 40 cm^{-1}	20
9. Synthetic Spectrum of 5.5μ - 8μ Emission Region for a Stark Field Corresponding to 10^{15} e's/cm ³ , a 6g - 5f, 6h - 6g Component Linewidth of 40 cm^{-1}	21

Tables

1. Infrared Emission Lines Observed in Oxygen From 5.5μ to 14μ	12
2. Emission Lines Predicted to Be Within the Experimental Width of the $7.43\mu\text{m}$ Emission Line at $T_D = 6\mu\text{s}$, $P_{O_2} = 176$ Torr	12

1. INTRODUCTION

Oxygen atom short wavelength infrared (SWIR) transitions observed in previous **Laser-Induced Nuclear Simulation (LINUS)** studies¹ originate in states which lie more than 6800 cm^{-1} below the ionization limit at 109837.02 cm^{-1} . These states are produced by collisional deactivation of higher-lying atomic states produced by three-body recombination of $\text{O}^+({}^4\text{S}^0)$ with electrons. For several reasons, spectroscopic observation of these higher-lying atomic states in a high-electron density, high-temperature plasma presents a formidable experimental challenge. Insofar as the plasma may be described by a time dependent temperature of some kind, the atomic state population will decrease as the principal quantum number n increases for a given orbital and spin angular momentum configuration. Since the energy separation between states decreases as n increases, collisional deactivation processes will be more efficient for higher-lying states than for lower-lying states. Even without the small separations in energy, higher- n states might have a larger cross-section for deactivation than lower states, due to the increasingly extended nature of their electronic wave functions. Infrared emission lines between O-atom states where $n > 4$ are expected to lie at progressively longer wavelengths, occurring in regions where detector technology is less well-developed than for the SWIR. The sum of these considerations has resulted in the lack of observations of **any** O-atom emission lines at wavelengths longer than $5\text{ }\mu$ in either plasmas or discharges. Although line positions and oscillator strengths have been calculated for O-atom infrared transitions based on experimentally and theoretically determined energy levels, an experimental comparison with these calculations is a matter of considerable importance for the understanding of the infrared radiation processes which might occur in the disturbed upper atmosphere. We report here the first time-resolved observations of transitions in the MWIR and LWIR in the $5\text{ }\mu - 14\text{ }\mu$ region from a recombining oxygen plasma. Assignments have been made for the

Received for publication 27 Dec 1985

transitions using experimental and calculated energy levels from the literature.^{2,3,4,5,6,7}

The strongest of the observed emission features occurs at 7.43μ . This feature has been studied as a function of background gas pressure and delay time, τ_D . The longest-wavelength infrared line transitions identified positively are $6h^{3,5}H \rightarrow 5g^{3,5}G^0$ and $6g^{3,5}G^0 \rightarrow 5f^{3,5}F$ calculated to be at 7.450μ and 7.426μ respectively. The oscillator strengths calculated by Biemont and Grevesse², and Sappenfield⁸ employing the Coulomb Approximation (CA) and our own hydrogenic calculations, are considered for a qualitative discussion of the relative intensities of the these emission lines. The observed 7.43μ emission feature occurs at the calculated position within experimental resolution. The observation of the $6g$ and $6h$ states suggests that lower-lying states which are predicted to give rise to LWIR emission are also populated, although we have not yet observed these lines for technical reasons.

2. EXPERIMENTAL

Figure 1 illustrates the experimental apparatus used for the MWIR emission studies. A Quanta-Ray Nd:YAG laser (model DCR 1A, $\lambda = 1.064 \mu$, 10 ns FWHM multilongitudinal pulse, 10 Hz repetition rate) was focussed with a 56 mm f.l. biconvex lens into a gas cell containing pressures of 50 to 250 torr O_2 . The laser was propagated parallel to the monochromator entrance slit. A typical average laser power of 4 W created an estimated intensity of $2 \times 10^{13} W cm^{-2}$ in the focal region.

The radiation from the laser-produced plasma was collected at 90° to the axis of the laser beam and collimated and focused on the spectrometer entrance slit using two 100 mm f.l. ZnSe lenses. In order to block all radiation except the wavelengths of interest from reaching the detector, a Corion Industries filter transmitting the wavelengths $5.3 - 9.0 \mu$

was placed just inside the entrance slit. The Spex 1870 spectrometer (0.5 m f.l.) was fitted with a 150 grooves/mm grating blazed at 6.0μ . Use of this grating with 3 mm slit widths yielded an overall resolution of 0.04μ . The detector was a Santa Barbara Research Center (SBRC) HgCdTe photoconductive chip mounted in a side-looking dewar cooled to 77 K, used in conjunction with a SBRC A110 preamplifier providing gain of 80 db. The system time response was 0.5μ s. Signal processing was done with a PAR 162-165 boxcar averager using a 1.5μ s gate. The output of the boxcar was recorded on a strip chart recorder.

The wavelength accuracy of the spectrometer was checked by collecting 1.064μ laser radiation scattered in 5th and higher orders. An additional check of MWIR line positions was carried out by replacing the MWIR bandpass filter with a germanium window which transmitted wavelengths $> 1.8 \mu$. This made possible the simultaneous viewing of SWIR lines in 2nd order along with the (much weaker) MWIR lines. The spectrum was calibrated using the line at 5.97μ and the 7th order of the 1.0642μ laser radiation with the 7.45μ line. LWIR scans were carried out using a 75 grooves/mm grating blazed at 10μ and a LWIR pass filter. The optical path was flushed with dry nitrogen or helium when spectra are taken in regions where water absorption is considered a problem. A search for emission lines using pure nitrogen gas in the same spectral region and under the same experimental conditions showed only continuum radiation. This negative result helps to confirm the origin of the oxygen plasma emission features as due to oxygen atoms and not artifacts of the gas handling system.

3. RESULTS

Figure 2 illustrates the 5.5μ - 8μ emission spectrum of a 150 torr laser-produced oxygen plasma with a 10μ s delay, uncorrected for the spectral response of the system, with 0.04μ resolution. In spite of the relatively slow time response of the detector, the setting of the 1.5μ s boxcar gate at 10μ s after the laser pulse proved to be sufficient to gate out the

early-time continuum emission. All observed lines originate in the O-atom levels with $n = 4, 5, 6$. The plasma temperature was estimated using the relative populations calculated from the intensity ratio of the 6.62μ and 5.97μ lines and found to be $4,000 \pm 1,000$ K. This estimate of a "temperature" is the only one available to us from our limited data. No line emission was detected above 7.45μ . Table I lists the observed infrared emissions along with observed linewidths, $\Sigma g f$ factors and line assignments.

Measurements were made on the 7.43μ emission as a function of delay after the plasma initiation and as a function of pressure. The linewidth (full width at half maximum, FWHM) obeys the following empirical relationship:

$$\Gamma(t, P) = 0.177P(\text{torr}) \cdot 3.31 \tau_D(\mu\text{s}) + 36.20 \text{ cm}^{-1}$$

with a standard deviation $\sigma = 1.39 \text{ cm}^{-1}$, where $\Gamma(t, P)$ is the linewidth in cm^{-1} , P is the pressure in torr, and τ_D is the observation delay time in μs , and where $50 < P(\text{torr}) < 200$, $4 < \tau_D(\mu\text{s}) < 20$. The linewidth data as a function of pressure and delay time are summarized in Fig. 3 and Fig. 4 for the 7.43μ transition.

1. DISCUSSION

These results constitute the first MWIR observations of line emission in a recombining oxygen plasma and the first observation of the $6h^{3,5}H \rightarrow 5g^{3,5}G^0$ emission. Several general conclusions may be drawn from the experimental observations:

1. The observed lines may be assigned exclusively to transitions between high-lying O-atom states. No emission attributable to O_2 or ionic oxygen is observed. Infrared emission between vibrational levels of ground states O_2 is electric dipole-forbidden. The plasma temperature is apparently sufficiently low so that very high-lying states of O^+ which might give rise to MWIR emission are not populated at our observation times. The ozone emission with origin at 9.5μ is absent. Emission is not observed from O-atom states with an O^+

($^2D^0$) core configuration.

2. The positions of the lines at 5.97μ , 6.61μ , 6.84μ , and 7.43μ correspond to calculated values to well within experimental resolution. The 5.74μ line center is slightly displaced from the calculated value of the $5d^5D^0 \rightarrow 5p^5P$ transition (5.68μ). The line center position is not reproducible from spectrum to spectrum because of poor signal-to-noise.
3. All of the observed lines are predicted to be strong by the CA calculations. No lines are observed which have low CA oscillator strengths. In addition, we might expect CA calculations to be even more justified for MWIR lines originating in $n = 5,6$ than for SWIR lines originating in $n = 4$. Therefore, we believe that CA calculations used in conjunction with tabulated energy levels differentiate accurately between strong and weak MWIR lines.

The preliminary nature of these data precludes addressing accurately the quality of the CA calculations for each of the individually observed lines. However, some qualitative discussion of the results along with some speculation may be offered. The "temperature" calculated from the $6.61 \mu/5.97 \mu$ intensity ratio gives a temperature of about 4,000 K. These lines were chosen for the temperature estimation since their upper states are subject to no known perturbations, allowing more reliance on the CA oscillator strengths. However, the np^3P states are known to be perturbed by close-lying levels.² The $5p^3P$ and $5p^5P$ states are separated in energy by 244 cm^{-1} , with the triplet state at higher energy, and would be expected to contain nearly equal populations under these temperature conditions. Since the $5p^3P$ state is observed to contain a lower population than the $5p^5P$ state by a factor of 0.6, we believe the true oscillator strength for the $5p^3P \rightarrow 5s^3S^0$ transition at 6.84μ ought to be lower than the calculated CA oscillator strength. Additional evidence for perturbation of the $5p^3P$ state is obtained by the lack of observation of the $5d^3D^0 \rightarrow 5p^3P$ transition at 6.49μ . This transition ($\Sigma gf = 13.1$) ought to be observed nearly as strongly as the $5d^5D^0 \rightarrow 5p^5P$ transition at 5.68μ in the absence of perturbations, yet is apparently missing. These data suggest that further attention taking account of detailed state-to-state

perturbations should be devoted to the calculation of all infrared oscillator strengths for lines which either originate or terminate in a $np\ ^3P$ state.

The broad emission feature centered at $7.43\ \mu$ is assigned predominantly to the $6g\ ^3,5G^0 \rightarrow 5f\ ^3,5F$ and $6h\ ^3,5H \rightarrow 5g\ ^3,5G$ transitions. The calculated oscillator strengths for these transitions are extremely high ($\Sigma gf = 66.1$ and 127 respectively) and the transitions are expected to appear quite strongly in spite of the high energy of the $6g\ ^3,5G^0$ and $6h\ ^3,5H$ states. These transitions are expected to be particularly sensitive to Stark broadening effects. due to the high n,l values of the states involved, the nearness of perturbing levels and the large polarizabilities of the states.

The position of the $6h\ ^3,5H$ term can be estimated using polarization theory.⁹ The result is $106,788.515\ \text{cm}^{-1}$ or about $0.6\ \text{cm}^{-1}$ above the $6g\ ^3,5G^0$ state. We may check this estimate by computing the position of the $5g\ ^3,5G^0$ term, at $105,445.962\ \text{cm}^{-1}$ previously assigned by Saum and Benesch⁴ Our estimate is $105,446.259\ \text{cm}^{-1}$. Using this calculated value for the term energy of the $6h\ ^3,5H$ state the $6h\ ^3,5H \rightarrow 5g\ ^3,5G^0$ transition is predicted to lie at $7.450\ \mu$, well within the envelope of the experimentally observed emission feature.

4.1 Linewidth

The range of observed linewidths for the emission lines is from $12\ \text{cm}^{-1}$ to $51\ \text{cm}^{-1}$ at a pressure of 176 torr and a delay time of $6\ \mu\text{s}$. The emissions at $5.97\ \mu$ and $6.61\ \mu$ are assigned as the single transitions $5p\ ^5P \rightarrow 5s\ ^5S^0$ ($17\ \text{cm}^{-1}$) and $5p\ ^3P \rightarrow 5s\ ^3S^0$ ($15\ \text{cm}^{-1}$), while the emission line at $7.43\ \mu$ is assigned as an envelope of a number of transitions dominated by the $6g\ ^3,5G^0 \rightarrow 5f\ ^3,5F$ and $6h\ ^3,5H \rightarrow 5g\ ^3,5G^0$ transitions. These widths are well outside the spectrometer resolution of about 2 to $4\ \text{cm}^{-1}$. The major contribution to the linewidth is expected to be due to interactions between the neutral atom and the electron density of the plasma. Therefore, a study and understanding of linewidths and shapes should lead to estimates of the electron number density in the plasma. Contributions to the

observed linewidths will be discussed in this section. First, a synopsis of line broadening will be given to establish notation.

4. 1. 1. HOMOGENEOUS BROADENING

The natural width of a particular transition is given in terms of the oscillator strength and wavelength by $\Gamma_{ki}(\text{cm}^{-1}) = |f_{ki}| / 450 \lambda_{ki}^2(\mu)$, where $|k\rangle$ represents the upper state and $|i\rangle$ the lower state of the atom. f_{ki} represents the emission oscillator strength and is related to the absorption oscillator strength by $f_{ki} = -(g_i/g_k)f_{ik}$ and to the transition matrix element by $|\langle i|r|k\rangle|^2 = -10.97 \lambda_{ki}(\mu)f_{ki}$ a.u. The g_i and g_k are lower state and upper state degeneracies respectively. The line strength is $S_{ik}(\text{a.u.}) = 32.92 g_i f_{ik} \lambda(\mu)$ and its relation to the Einstein coefficient is $A_{ki}(\text{s}^{-1}) = 2.03 \times 10^6 S_{ik}/g_k \lambda^3(\mu)$ where S_{ik} is in atomic units. The intensity in watts/atom-steradian is defined as $J_{ki} = (3.013 \times 10^{-13} \lambda^4(\mu))|\langle i|r(\text{a.u.})|k\rangle|^2$. The sum of all the allowed transitions between the $6g^5G_J^0$ and the $5f^5F_J$ states gives $|f_{ki}| = 4.705$ yielding a width $\Gamma = 0.002 \text{ cm}^{-1}$, a lifetime $\tau_0 = 176 \text{ ns}$ and a halflife $\tau_{1/2} = 122 \text{ ns}$.

We may estimate the cross-section necessary to account for lifetime broadening due to non-radiative processes using estimated properties of a typical plasma system. For velocities corresponding to temperatures of 2500 K to 4500 K, $n_e = 10^{16} \text{ electrons/cm}^3$ and a linewidth of 12 cm^{-1} the cross-section would have to be approximately 10^{-13} cm^2 .

4. 1. 2. INHOMOGENEOUS BROADENING

Within the observed line profile of the 7.43μ emission there are a number of possible transitions so that we might consider the emission profile as an electron broadened composite of these. Table II lists these transitions. Figure 7 shows a simulation of the lines from 5.5μ to 8.0μ using CA intensities, an instrument resolution of 4 cm^{-1} , a linewidth of 12 cm^{-1} for all lines except the $6h-5g$ and $6g-5f$ transitions which were assigned a 40 cm^{-1} width.

4.2 Stark Lineshape Theory

In order to gain further understanding of the broadness of the 7.45μ feature, we have synthetically constructed an emission profile based on computed oscillator strengths and a simple non-degenerate Stark broadening theory. The matrix elements computed in this theory may be used later in a more extensive theory of line broadening. We assume that the emitting atom experiences an average electric field which is computed using the electron density as a parameter. For simplicity we ignore the Holtsmark distribution function. This average field splits the J-sublevels of a given term to second order in the Stark effect.

The Stark shift ΔE_{nJLS} is given in second order by

$$\Delta E_{nJLS} = \Sigma_{n'J'L'} \frac{|\langle n'J'L'S|R(1)|nJLS \rangle|^2}{E_{n'J'L'S}^{(o)} \cdot E_{nJLS}^{(o)}}$$

where a sum over spatial orientation has already been performed and a sum over 17 terms for each multiplicity has been taken. The matrix elements,

$$|\langle n'J'L'S|R(1)|nJLS \rangle|^2 = ((2J+1)(2J'+1)(2L+1)(2L'+1)) \\ \times |\langle (n'L')|R(1)|(nL) \rangle|^2 \begin{Bmatrix} S & J' & L' \\ 1 & L & J \end{Bmatrix}^2 \begin{Bmatrix} L' & 1 & L \\ 0 & 0 & 0 \end{Bmatrix}^2$$

where $\langle (n'L')|R(1)|(nL) \rangle$ represents the integration over the radial wave function of the atom and the usual notation for 3j and 6j symbols is used.¹⁰ These matrix elements are calculated using hydrogenic wave functions and agree reasonably with the CA results. The width, Γ , and shift, Δ , of each J-component in each term is assumed to be due to electron collision processes. We may scale the temperature and electron number density dependence of this width¹¹ using

$$\Gamma = (1 + 1.75a(n_e)(1 - 0.75R(n_e)))\Gamma_0$$

$$\Delta = (\Delta_0/\Gamma_0 + 2.0a(n_e)(1 - 0.75R(n_e)))\Gamma_0$$

where $a(n_e)$ = the quasi static ion broadening parameter, $R(n_e)$ = the Debye shielding parameter, and where a scales as $n_e^{1/4}$ and Δ and Γ scale as n_e . Alternatively, a width parameter set by the observed width of a single, isolated transition may be introduced. The energies of the perturbing levels are taken from Bashkin³, Saum and Benesch,⁴ Erickson and Isberg,⁶ Isberg⁷ and Russell-Saunders coupling is assumed. It should be noted that the $6g^{3,5}G^0$ state is only 0.6 cm^{-1} below the $6h^{3,5}H$ level and 2.8 cm^{-1} above $6f^{3,5}F$. We also assume that the effective electric fields have no preferred direction in space. The second-order Stark effect connects levels by way of dipole matrix elements. These have been calculated using hydrogenic wave functions and the matrix elements compared with previous calculations.^{2,12,8,13} The Stark calculation estimates the perturbation of each J-sublevel in a given term and computes the wavelengths and energies for transitions between terms. The relative intensities for each J-component are used to make up the line profile and the line shift comes about from the shift in the center of gravity of the resulting transitions. In this model, the 7.43μ emission feature is composed of the Stark splitting of each of the lines listed in Table II using the electron density as a parameter. Synthetic spectra are composed of Gaussian lineshapes having a width as previously described. An obvious feature of the synthetic spectra is the sensitivity on electric field strength. This is due to the presence of nearby perturbing levels. Results for electron densities of 10^{14} and 10^{15} cm^{-3} are presented in Figures 8 and 9. Clearly, the line positions of the calculated transitions are strongly influenced by the presence of an electric field. Since we observe no shift of line position from the zero-field predictions we conclude that either the electric field strength at the site of the emitting atoms is negligible, or that there is significant mixing of states so that a degenerate broadening theory should be used. The observed broadness of the 7.43μ feature must be due to a process essentially unrelated to the Stark J-level

splitting approach used for our spectral simulations.

Lifetime broadening could conceivably account for much of the observed width of the 7.43μ feature. A width of 50 cm^{-1} corresponds to a lifetime of 10^{-13} s . This implies the existence of an extremely efficient electron-emitter collision process. The decrease in linewidth with increasing time delay and decreasing pressure are consistent with this suggestion. Since the 6f, 6g and 6h states lie within an extremely narrow (3 cm^{-1}) energy range, the cross-section for collisional transfer between these states might be expected to be several orders of magnitude greater than gas-kinetic. Although it is difficult to assess the form of the potential which might be responsible for such rapid collisional state scrambling, it might prove significant that the hydrogenic matrix elements $\langle 6f|r|6g \rangle$ and $\langle 6g|r|6h \rangle$ are extremely large. In a sense, electron broadening is such a collision process. We are therefore applying a more rigorous lineshape theory to the near degenerate state situation found in the upper levels of atomic oxygen.

We have searched for O-atom line emission in the $8 \mu - 12 \mu$ region, with negative results. The CA oscillator strengths predict transitions in the 10.4μ and 11.7μ regions with oscillator strengths similar to the transitions observed in this experiment. These transitions originate in the levels $6d^5D$, $5p^3P$ and $6d^3D$. Since we observe $6g - 5f$ transitions in the MWIR, lower populations of levels giving rise to LWIR transitions should not be the cause of the failure to observe these lines, since the 6g levels lie higher in energy than the other levels. Rough calculations taking into account the lower energy of the LWIR transitions and the increase toward longer wavelengths of 300K background radiation viewed by the detector indicate that an increase in signal-to-noise ratio of at least a factor of 10 might be necessary for the laboratory observation of these LWIR emission lines. Several experimental parameters might be altered in order to obtain this signal-to-noise improvement. These include trading off detector time response for greater quantum

efficiency, increasing the laser repetition rate, lengthening the time width of the boxcar gate and performing slower spectrometer scans.

observed emission λ (μ)	linewidth Γ (cm $^{-1}$)	transition	calculated wavelength λ (μ)	Σgf_{ki}
5.74	51	5d $^5D^0$ - 5p 5P	5.6813	19.3
5.971	12	4p 5P - 3d $^3D^0$	5.9713	3.9
6.607	17	5p 5P - 5s $^5S^0$	6.6248	9.4
6.841	15	5p 3P - 5s $^3S^0$	6.8567	5.8
7.447	48	6g $^{3,5}G^0$ - 5f $^{3,5}F$ 6h $^{3,5}H$ - 5g $^{3,5}G^0$	7.4281 7.4501	66.1 127

Table I. Infrared emission lines observed in oxygen from 5.5 μ to 14 μ . Wavelengths and widths were measured at a pressure of 176 torr in pure oxygen with a 6 μ s delay.

λ (μ)	transition	Σgf_{ki}	J_{ki}	lower state (10 $^{-13}$ W atom)	short wavelength channel	final state	τ (ns)
				(cm $^{-1}$)	λ (μ)		
7.1419	5d $^5D^0$ - 6p 5F	18.7	440	105,385	1.0679	3d $^5D^0$	82
7.1739	5p 5P - 6s $^5S^0$	6.4	151	103,627	0.5437	3p 5P	328
7.2664	5d $^3D^0$ - 6f 3F	11.7	280	105,409	1.0754	3d $^3D^0$	143
7.426	6g $^5G^0$ - 5f 5F 6g $^3G^0$ - 5f 3F	41.4 24.7	1012 604	105,442	-	-	-
7.450	6h 5H - 5g $^5G^0$ 6h 3H - 5g $^3G^0$	45.3 82.2			-	-	-
7.5052	7f 3F - 11d $^3D^0$.057	1.4	107,595	-	-	-
7.5236	6f 3F - 8d $^3D^0$.20	4.9	106,785	0.5131	3p 3P	-
7.550	5f 3F - 6d $^3D^0$.614	15.3	105,442	0.0973	ground	-
7.5683	6f 5F - 8d $^5D^0$.40	10	106,785	-	-	-
7.6323	5f 5F - 6d $^5D^0$	1.2	30.2	105,442	0.4967	3p 5P	-
7.7186	5p 3P - 6s $^3S^0$	4.0	101	103,870	0.0951 0.6046	ground 3p 3P	- 1280

Table II. Emission lines predicted to be within the experimental width of the 7.43 μ m emission line at τ_D = 6 μ s, P_{O_2} = 176 torr.

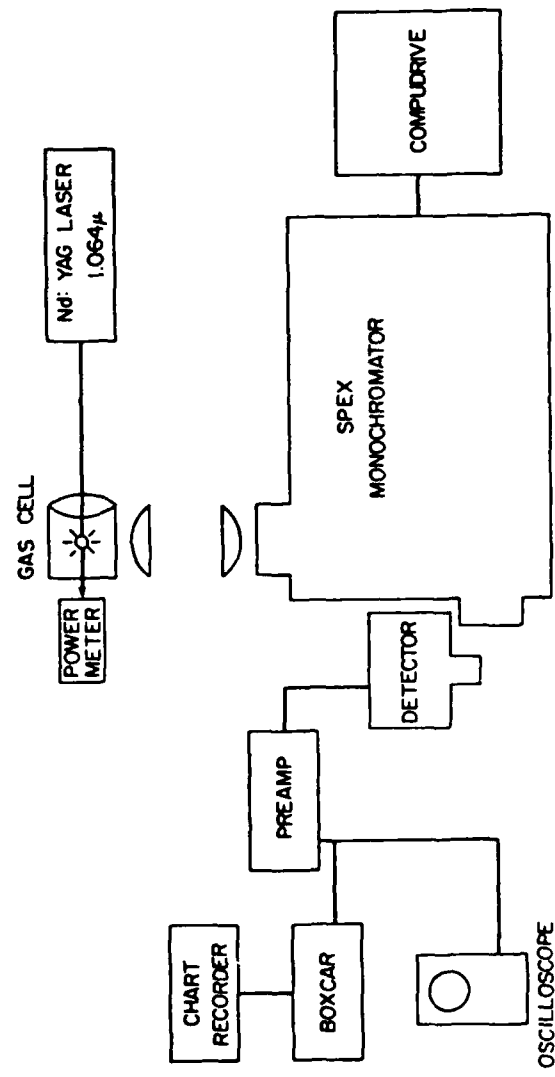


Figure 1. Experimental Apparatus for Infrared Emission Studies

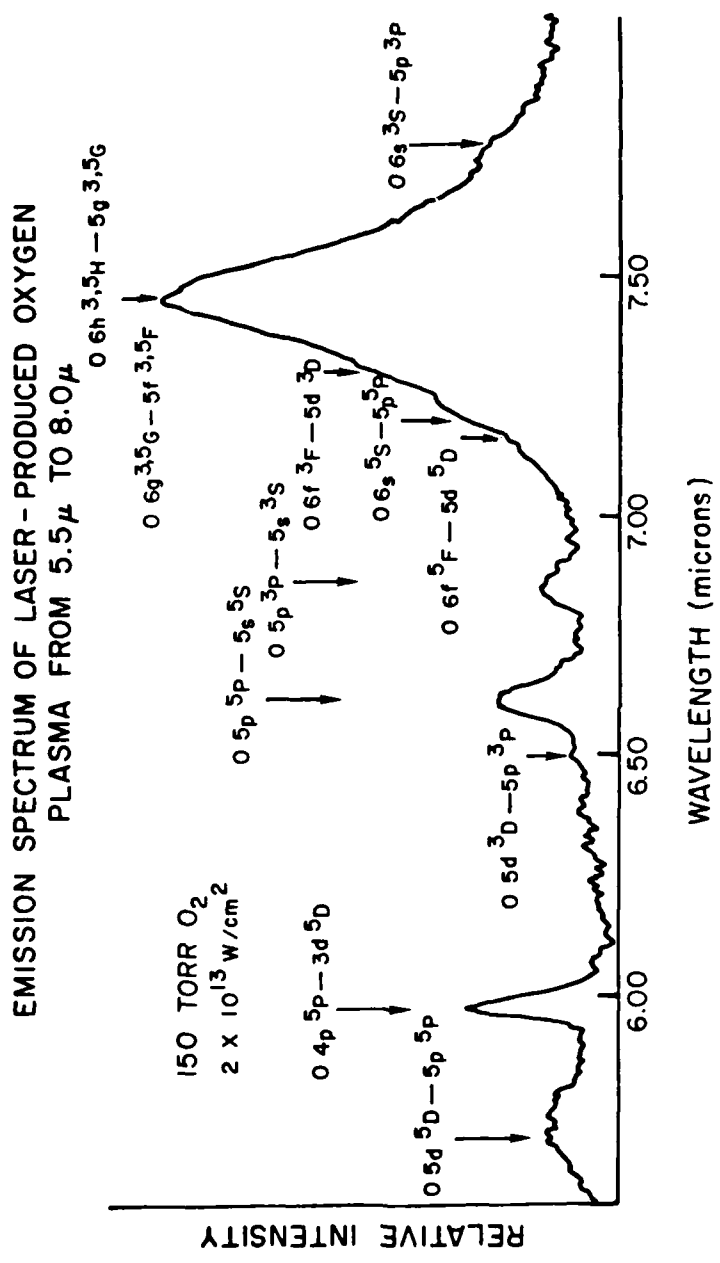


Figure 2. $5.5\mu - 8\mu$ emission spectrum of a 150 torr laser produced oxygen plasma with
 a $10\mu\text{s}$ delay.

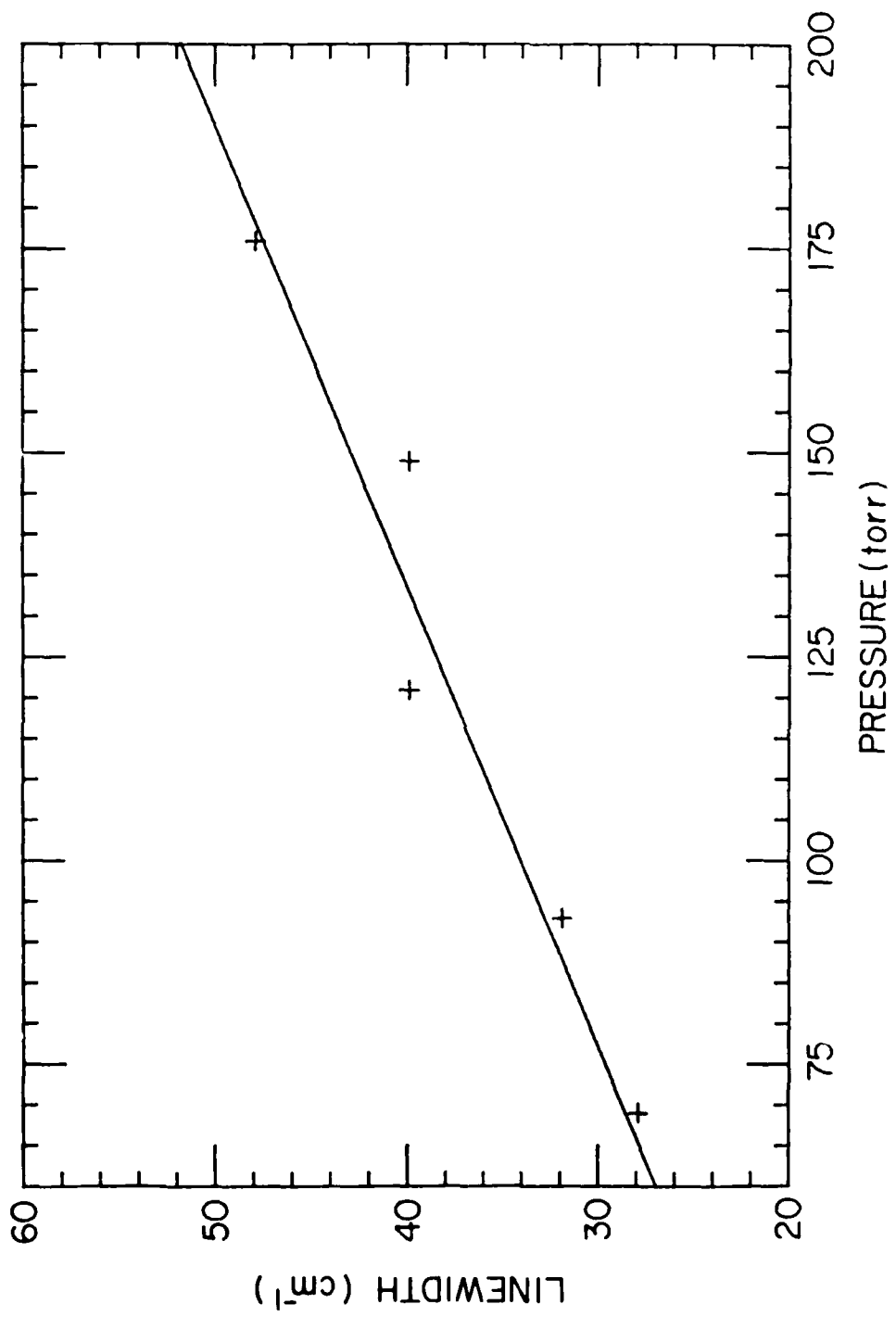


Figure 3. 7.43μ emission linewidth vs. total oxygen pressure at $\tau_D = 6 \mu$ s.

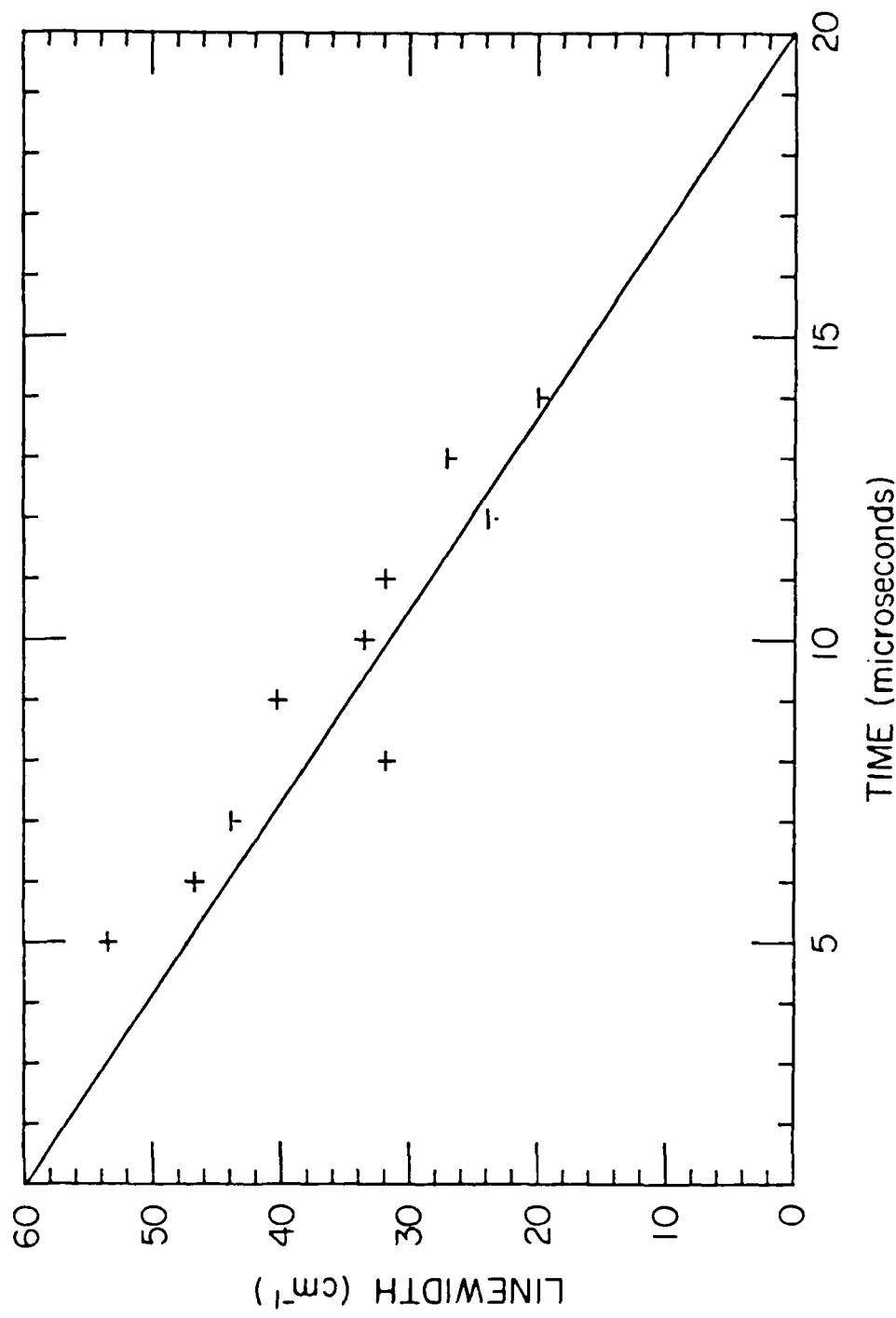


Figure 4. 7.43μ emission linewidth vs. τ D at 176 torr oxygen pressure.

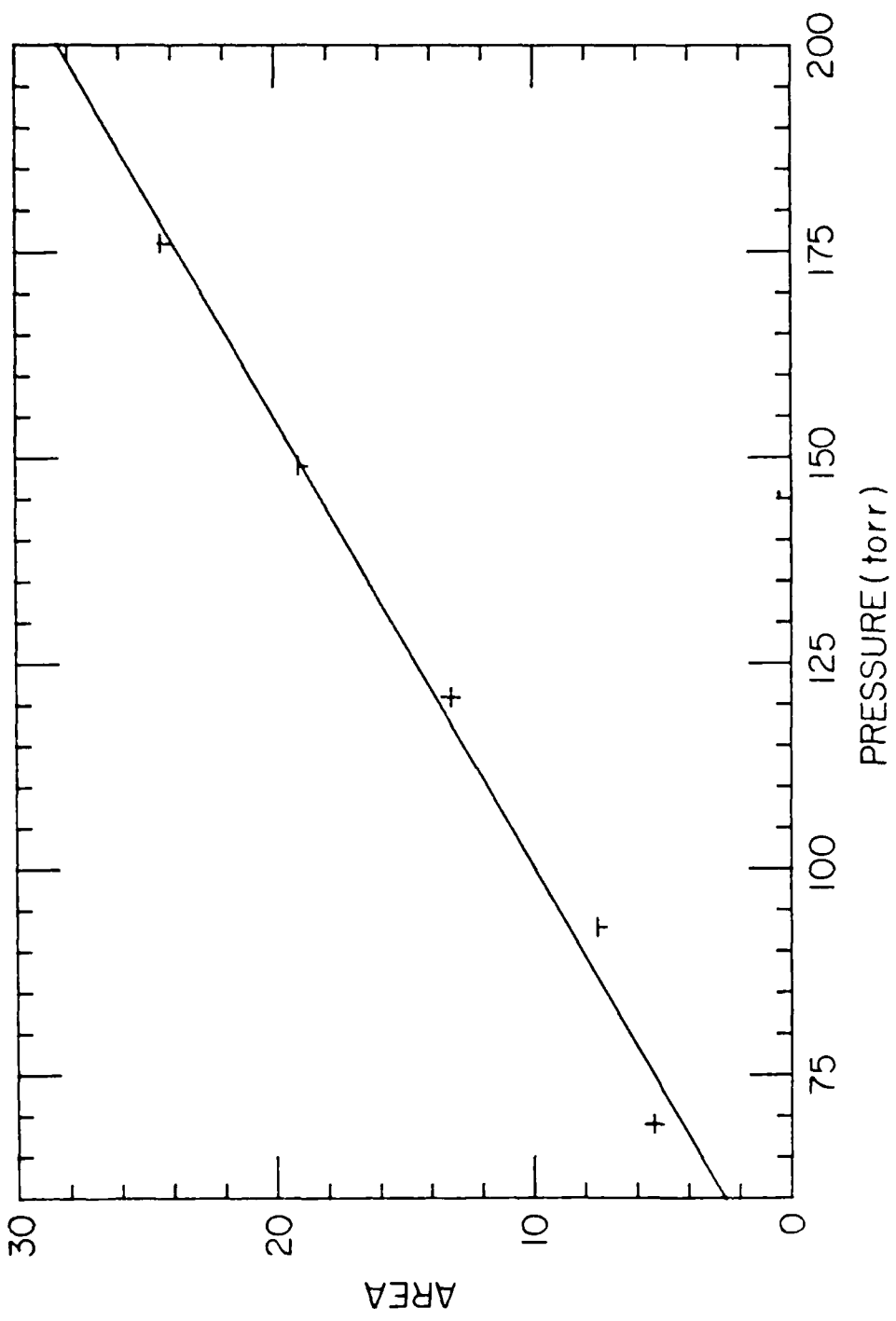


Figure 5. 7.43μ emission line area vs. total oxygen pressure at $\tau_D = 6 \mu$ s.

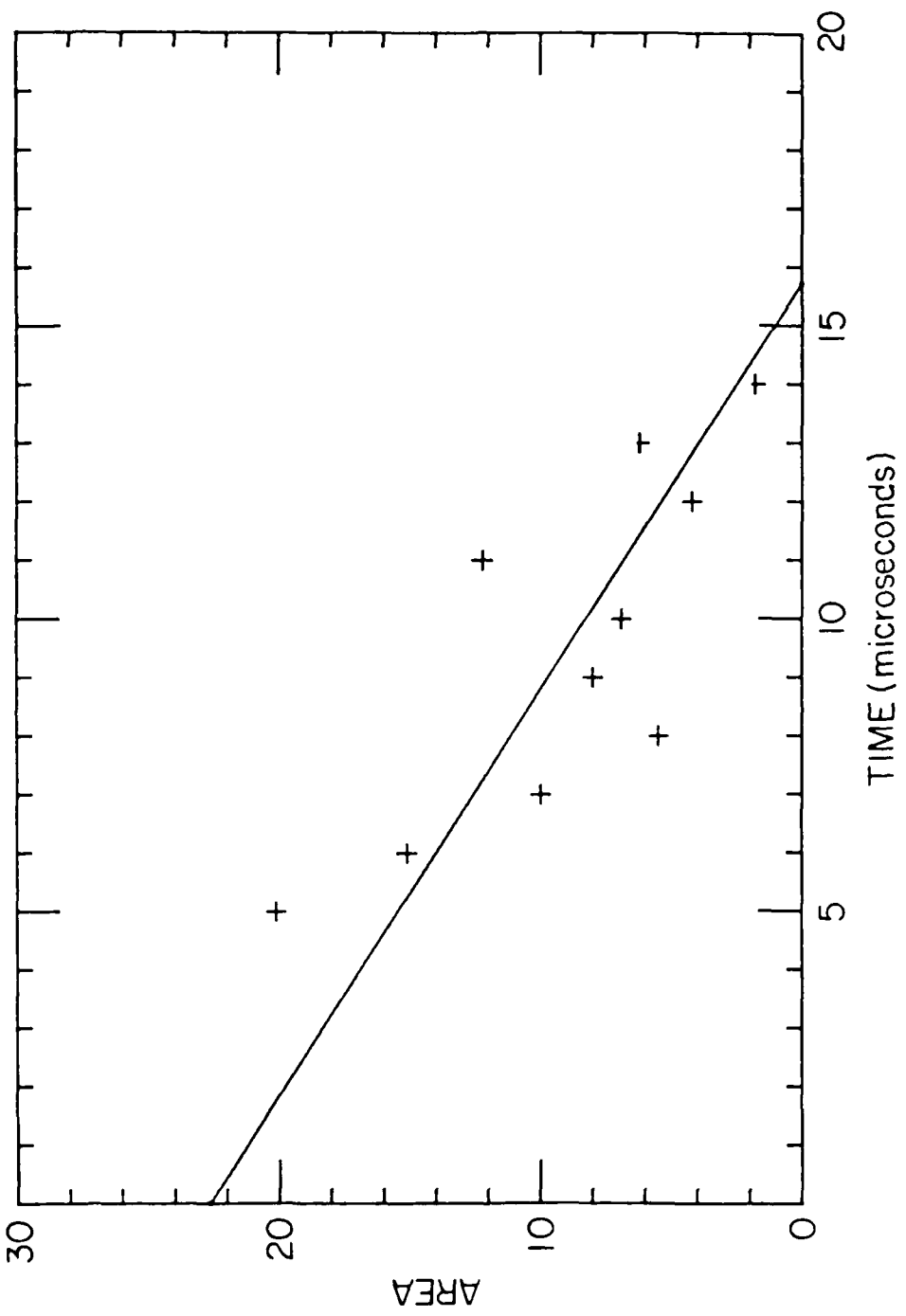


Figure 6. 7.43μ emission line area vs. τ_D at total oxygen pressure of 176 torr.

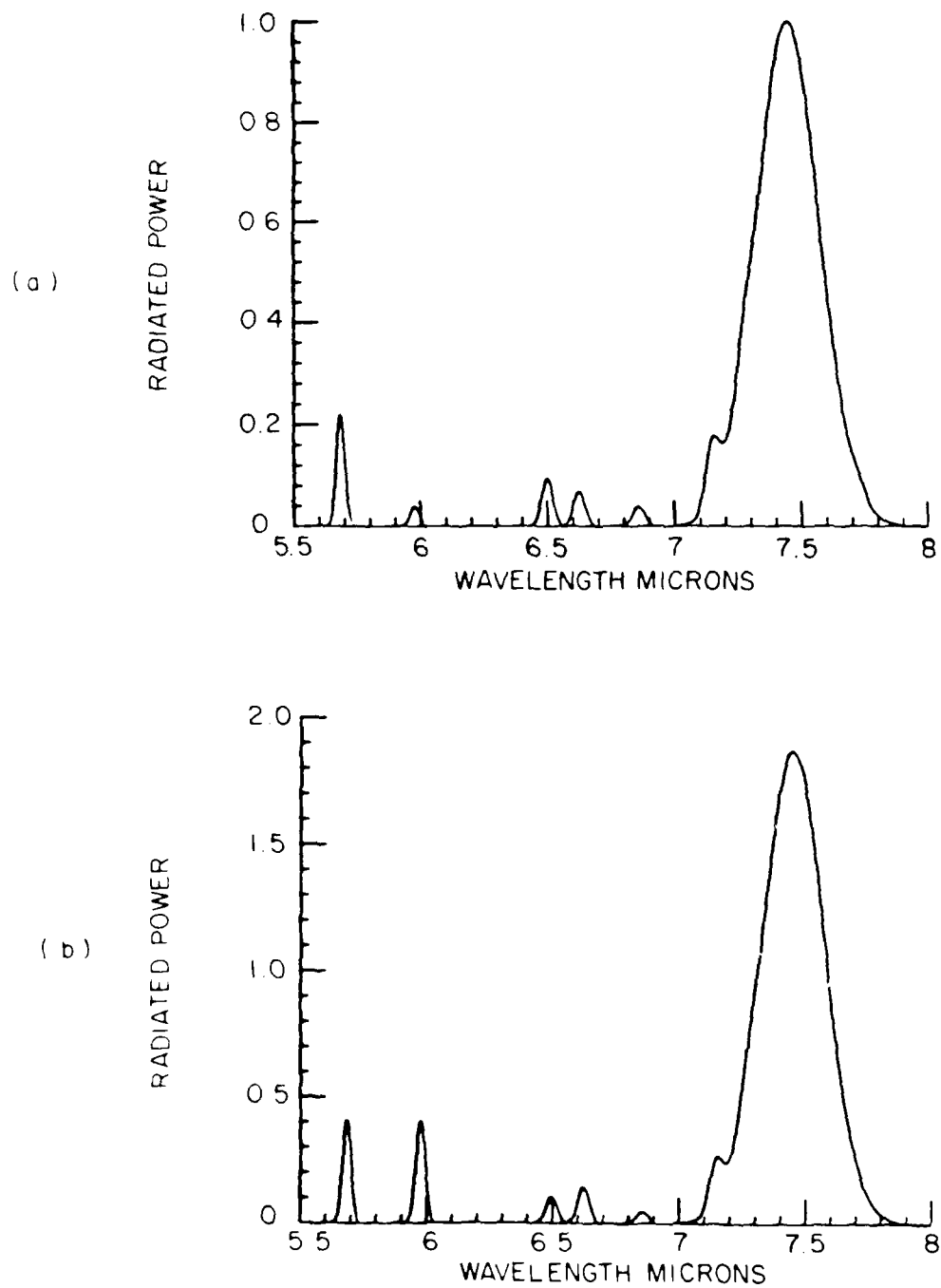


Figure 7. Simulated emission spectrum in the 5.5μ - 8.0μ region using Coulomb Approximation intensities, 40 cm^{-1} widths for the $6g$ and $6h$ states and 12 cm^{-1} linewidths for the rest of the transitions. (a) Equal population of states assumed. (b) A Boltzmann distribution at a temperature of 4000 K is assumed among 36 terms of interest.

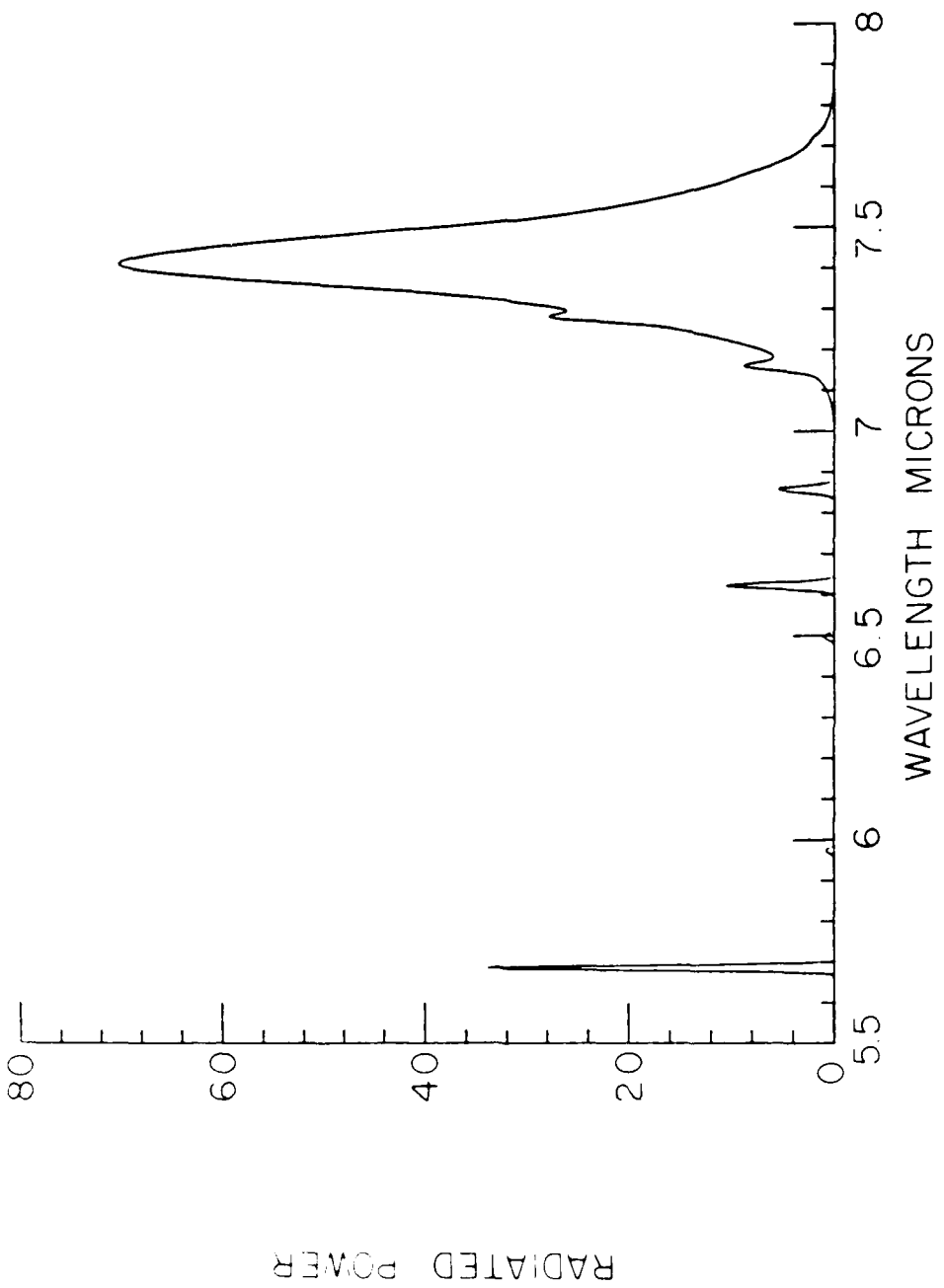


Figure 8. Synthetic spectrum of $5.5 \mu - 8 \mu$ emission region for a Stark field corresponding to 10^{14} e's/cm^2 , a $6g - 5f$, $6h - 6g$ component linewidth of 40 cm^{-1} .

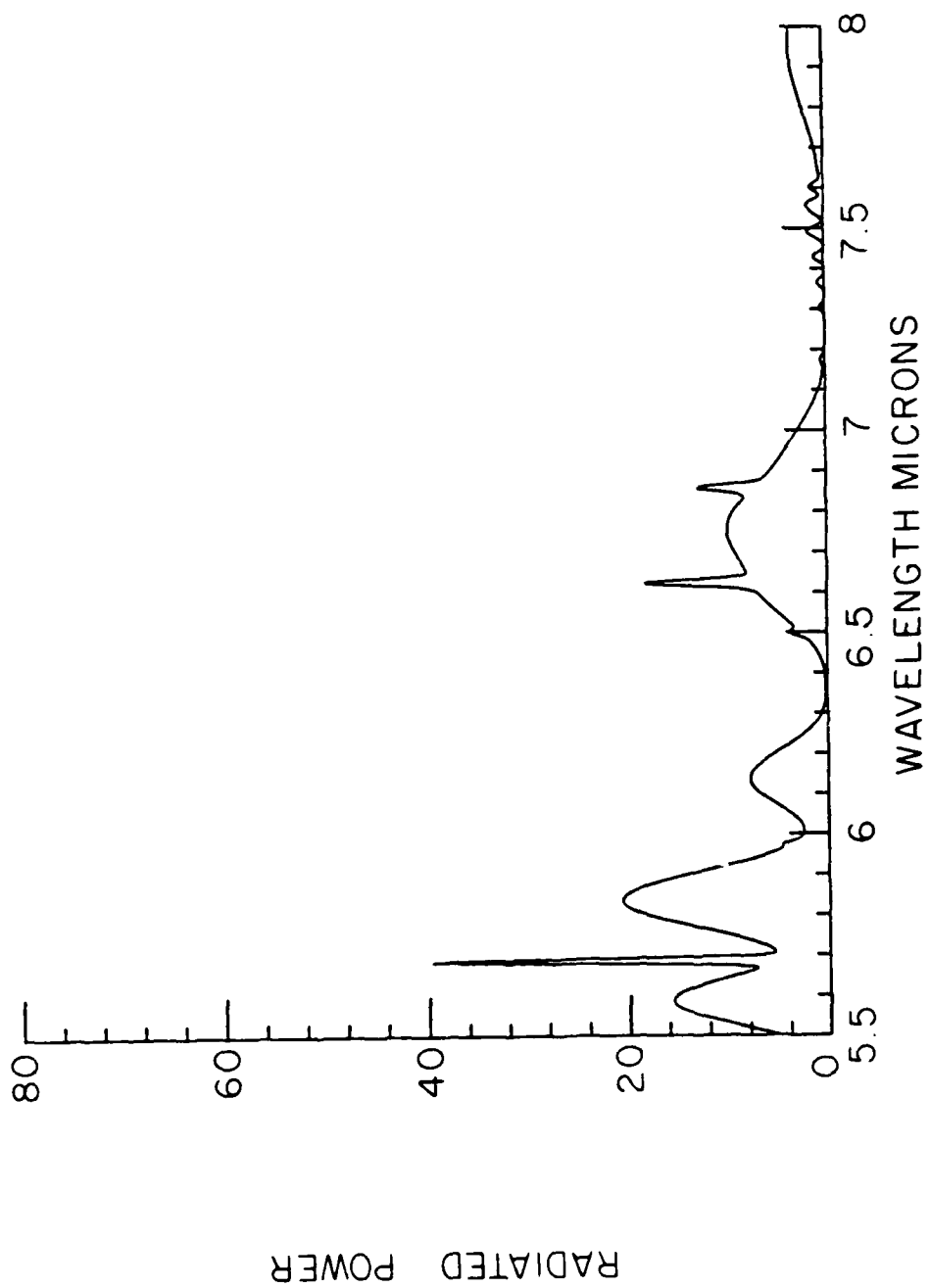


Figure 9. Synthetic spectrum of $5.5 \mu - 8 \mu$ emission region for a Stark field corresponding to 1015 eV/cm^2 , a $6g - 6f$, $6h - 6g$ component linewidth of 40 cm^{-1} .

References

1. J. Lurie, S. Miller, R. Armstrong, Technical Report AFGL-TR-84-0161, (1984), AD A147528.
2. E. Biemont and N. Grevesse, *Atomic Data and Nuclear Data Tables* **12**, 217, (1973).
3. S. Bashkin and J.O. Stoner, *Atomic Energy Levels and Grotian Diagrams*, Vol. I, North Holland Publishing Co., N.Y. 1975
4. K. A. Saum and W. M. Benesch, *Applied Optics* **9**, 1419 (1970)
5. C. E. Moore, *Atomic Energy Levels*, Vol. I, NBS **467**, (1949).
6. K. B. S. Eriksson and H. B. S. Isberg, *Arkiv För Fysik* **24**, 549 (1963)
7. B. Isberg, *Arkiv För Fysik* **35**, 495 (1967)
8. D. Sappenfield, *private communication*
9. B. Edeln, *Handbuch der Physik*, **27** sec. 20, (1964).
10. A. R. Edmonds, *Group Theory and Quantum Mechanics*, Princeton University Press 1972.
11. H. R. Griem, *Plasma Spectroscopy*, McGraw Hill, N.Y. 1964; H. R. Griem, *Spectral Line Broadening by Plasmas*, Academic Press, N.Y.
12. A. K. Pradham and H.G. Saraph, *J. Phys. B: Atom. Molec. Phys.* **10**, 3365, (1977)
13. H.B. Schulman, F. A. Sharpton, S. Chung, C. C. Lin, and L. W. Anderson, to be published.

E N D

D T I C

8-86